

WIND EFFECT ON MILAD TOWER USING COMPUTATIONAL FLUID DYNAMICS

MAHMOUD YAHYAI*, AMIR SAEDI DARYAN, SEYED MASOUD MIRTAHERI
AND MASOUD ZIAEI

Department of Civil Engineering, K.N. Toosi University Of Technology, Tehran, Iran

SUMMARY

Milad tower is located in Tehran, Iran, and is a 436-m telecommunication tower ranked as the fourth tallest structure in the world. Because of its specific use and also because of highly sensitive communication devices installed on the tower, nonlinear deformations under future severe winds and earthquakes should be studied. In this paper, a comprehensive study is carried out to investigate the effect of wind on this tower. The techniques of computational fluid dynamics, such as large eddy simulation (LES), Reynolds Averaged Navier–Stokes Equations (RANS) model and so on, were adopted in this study to predict wind loads on and wind flows around the building. The calculated results are compared with those of wind tunnel test. It was found through the comparison that the LES with a dynamic subgrid-scale model can give satisfactory predictions for mean and dynamic wind loads on the specific structure of Milad tower, while the RANS model with modifications can yield encouraging results in most cases and has the advantage of providing rapid solutions. Furthermore, it was observed that typical features of the flow fields around such a surface-mounted bluff body standing in atmospheric boundary layers can be captured numerically. Copyright © 2009 John Wiley & Sons, Ltd.

1. INTRODUCTION

Computational wind engineering as a branch of computational fluid dynamics (CFD) has been developed rapidly over the last three decades to evaluate the interaction between wind and structures numerically, offering an alternative technique for practical applications. The techniques of CFD, such as large eddy simulation (LES), Reynolds Averaged Navier–Stokes Equations (RANS) model, etc., have been widely used to predict wind flows around bluff bodies in wind engineering. However, as reviewed by Murakami (1998), in the analysis of wind flow around a sharp-edged bluff body, there are many difficulties that do not appear in the usual CFD computations for simple flows. The difficulties in applying CFD to wind engineering problems are mainly caused by the following factors: (a) a large Reynolds number; (b) impinging at the front; (c) sharp edges of bluff bodies; (d) remaining effect of flow obstacle at outflow boundary, etc. Many efforts have been devoted to overcome these difficulties in recent years, which will be briefly mentioned below. The first effort was made on the revision of the RANS model, especially for the standard $k - \varepsilon$ model, since this kind of model has a good reputation for its efficiency and easy implementation. It has been recognized that the widely used standard $k - \varepsilon$ turbulence model can predict the general wind conditions around buildings reasonably well except those in the separation regions above roof surfaces and near side walls (Li *et al.*, 1998). This can be attributed to the overestimation of turbulence energy in the windward corner region by such a model. Therefore, two kinds of revised $k - \varepsilon$ model were proposed to improve its performance for predicting wind flows around bluff bodies. One was proposed by Launder and Kato (1993),

*Correspondence to: Mahmoud Yahyai, Department of Civil Engineering, K.N. Toosi University of Technology, Valiasr Ave. Tehran PO Box 15875-4416, Iran. E-mail: yahyai@kntu.ac.ir

and the other was presented by Murakami *et al.* (1998), which were called the Launder and Kato (LK) model and the Murakami, Mochida, Kondo (MMK) model, respectively. The LK model is aiming at the elimination of turbulence overproduction at the impinging region of bluff body flows by replacing the original production term $P_k = C_\mu \varepsilon S^2$ with $P_k = C_\mu \varepsilon S \Omega$, where $S = \frac{k}{\varepsilon} \sqrt{\frac{1}{2}(U_{i,j} + U_{j,i})^2}$ and $\Omega = \frac{k}{\varepsilon} \sqrt{\frac{1}{2}(U_{i,j} - U_{j,i})^2}$ denote, respectively, the strain and vorticity invariants. This revision is very simple and successful, with a slight increase of Central Processing Unit (CPU) time in computation. However, Murakami (1998) commented that it has a drawback of giving an overproduction of turbulence than the standard $k - \varepsilon$ model when $\Omega > S$. A new revised $k - \varepsilon$ model was thus proposed (Murakami *et al.*, 1998), i.e. the MMK model, which adds the modification to the expression of eddy viscosity ν_T instead of P_k . This may overcome the drawback of the LK model. In general, it gives better results than the LK model in the simulation of wind flows around a standard cube and a low-rise building model (Murakami *et al.*, 1998). Both the LK and MMK models have been used in wind engineering applications due to their simplicity and efficiency. However, with the advance of computational resources in recent years, more complicated techniques such as LES have attracted more and more attention in wind engineering. The LES is capable of simulating complex unsteady turbulent flows around a bluff body, which is very useful for investigating wind-induced vibrations of buildings and structures. Murakami (1998) reviewed the state-of-the-art LES applications in wind engineering and commented that the LES with a dynamic subgrid-scale (SGS) model is a promising tool for accurately predicting the flow field around a bluff body compared with other turbulence models. Rodi (1997) compared the LES and RANS calculations of vortex-shedding flows past a square cylinder at $Re = 22000$ and a surface-mounted cube at $Re = 40000$. He concluded that the $k - \varepsilon$ model strongly under-predicted the periodic motion due to the excessive turbulence production. The LK modification and two-layer approach resolving the near-wall region can give improved results but enlarge the length of the separation region behind the cube. It was observed that the LES can basically simulate all the complex features of three-dimensional flow past a surface-mounted cube fairly well, at the price of paying a larger computational effort. However, there are still some limits for the LES to be applied effectively in solving practical problems in wind engineering. The first limit is the SGS model. In fact, a variety of SGS models have been proposed, including the classic Smagorinsky model established by Smagorinsky (1963), the dynamic Smagorinsky–Lilly model developed by Germano *et al.* (1991) and revised by Lilly (1992), the wall-adapting local eddy viscosity model proposed by Nicoud and Ducros (1999), and the dynamic SGS kinetic energy model presented by Kim and Menon (1997). But strictly speaking, none of these SGS models are fully satisfactory. In order to obtain accurate simulation results of wind flows around bluff bodies, especially for the cases with a high Reynolds number, a suitable SGS model should be carefully chosen. The second limit is the near-wall treatment. Full solution of near-wall turbulence of a bluff body needs a very fine grid resolution, especially for separated boundary-layer flows, which makes a full-scale LES often inapplicable due to the huge amount of mesh numbers required. The third limitation is computational power, although it has been greatly developed in recent years. Up to now, the LES studies of bluff body flows are still restricted in moderate Reynolds number (10^4) ranges. Reliable and high-quality numerical works on bluff body flows with Reynolds number greater than 10^5 have rarely been reported. Obviously, there is a need to conduct intensive research work on this research. Considering the mentioned problems and since few studies have been carried out to investigate the accuracy and efficiency of different techniques of numerical wind tunnel simulation for the evaluation of wind effect on geometrically complicated structures, in the present study, an attempt was made to simulate boundary-layer turbulent wind flow around the Milad tower, as it is a structure with several geometrical surface complications. ANSYS (ANSYS Inc. Canonsburg, PA, USA) finite-element programme is used, which can carry out CFD analysis. A complete comparison is made between the two methods of boundary

condition turbulence simulation techniques, i.e. the LES method and the RANS method with the standard $k - \varepsilon$ model.

Furthermore, the main purposes of this study are the efficient simulation of the effect of wind with a high Reynolds number value and the development of a proper turbulence model to obtain reliable results for engineering applications. In the following sections, the structure of Milad tower is briefly described since this tower is selected to study the effect of wind on complicated structures.

2. STRUCTURE OF THE MILAD TOWER

The Milad tower consists of four main parts, namely the foundation, concrete shaft, head structure and the antenna.

2.1 Foundation

The foundation of the tower consists of two parts: the circular mat foundation and the transition structure. The diameter of the mat foundation is 66 m, and the thickness is varied between 3 and 4.5 m. The foundation is placed from height level of -14 m to height of -11 m at the center and -9.5 m at the corners of the foundation. The transition structure is an incomplete pyramid placed on the foundation and continued to height level of 0.0 m. The diameter of the transition structure is 49.6 m at the height level of -9.5 m and is equal to 28 m at ground level.

2.2 Concrete shaft

The concrete shaft is the main load-carrying structure of the tower that transfers all of the lateral and gravitational loads to the foundation. This structure begins from the height level of 0.0 m to the height level of 315 m. The diameter of the concrete shaft decreases from bottom to top.

2.3 Head structure

The head structure begins at the height level of 247 m to the height level of 315 m. It is placed around the concrete shaft and forms a 12-storey structure. The head structure consists of the following parts: the radial and peripheral, beams, columns, the basket and the concrete cone.

2.4 Antenna

The antenna is installed from the level of 308 m to the height level of 436 m. Different parts of Milad tower are shown in Figure 1.

3. MATERIALS AND METHODS

3.1 Calculation domain and mesh arrangement

The size of the model developed in this study is 1:100 scaled model of the Milad tower. Calculation domain, coordination and boundary conditions used in this study are shown in Figure 2.

As shown in Figure 2, the computational domain covers $30 D_y$ (D_y is the width of the tower) in stream-wise (X) direction ($-6 < x/D_y < 22$), $16 D_y$ in lateral or normal (Y) direction ($-8 < y/D_y < 8$) and $2 H$ in vertical (Z) direction. The reason for such a choice is to eliminate the flow-obstacle effect on the inflow and outflow boundary conditions, as discussed by Murakami *et al.* (1998). Considering the general shape of the tower shown in Figure 1 and the geometry of the tower structure, its computational mesh generation is not straightforward with regard to the boundary-layer conditions and wind

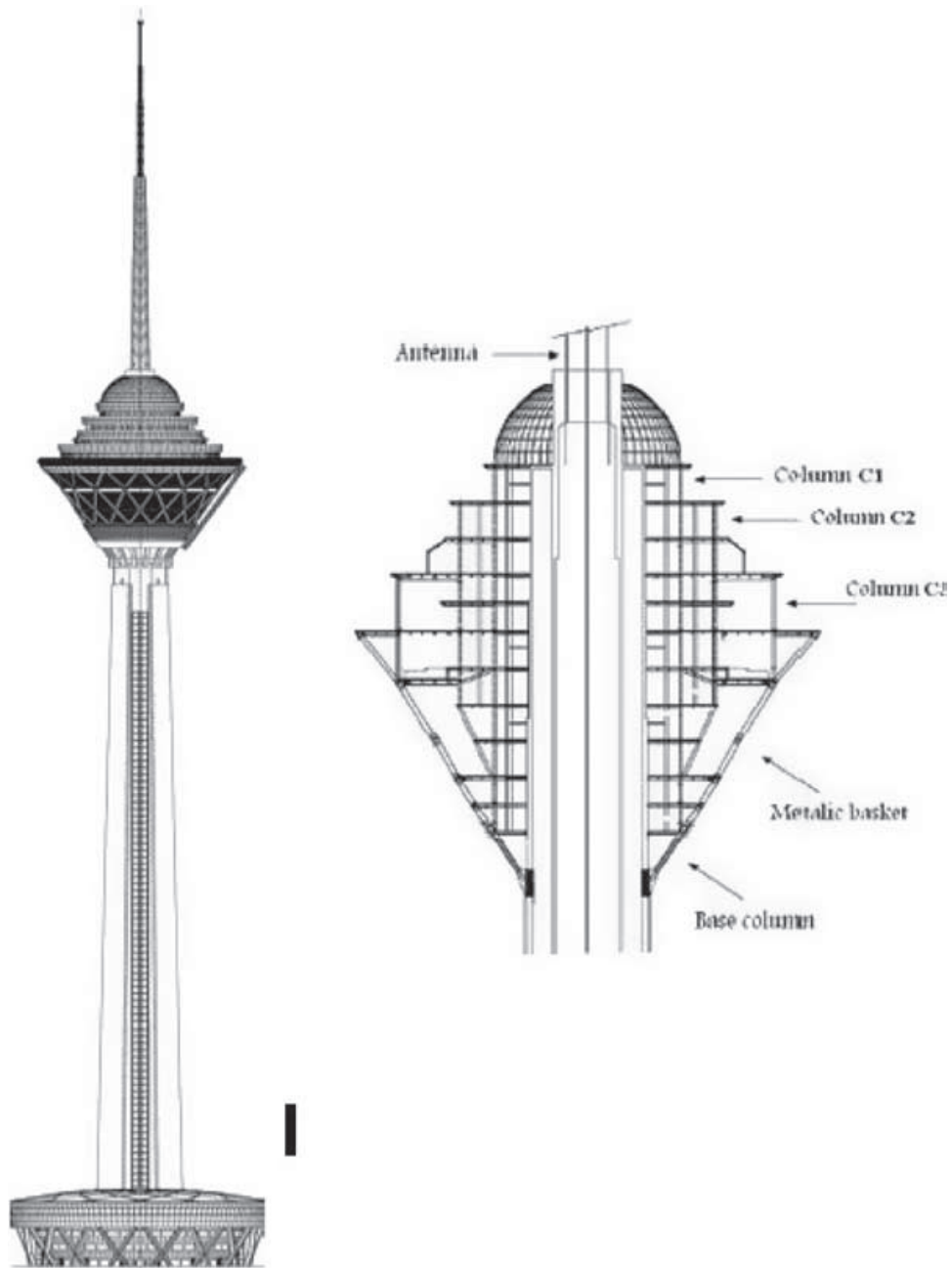


Figure 1. Different parts of the Milad tower

attack angle. Besides, the mesh number must be as low as possible to obtain an efficient computation. The traditional finite-element method uses a structured grid that requires a body-fitted grid transformation from physical domain to computational domain. The mesh near and aligned with the wall surfaces must be refined and stretched with a viscous boundary-layer grid. Figure 3 shows the modelling and mesh arrangement.

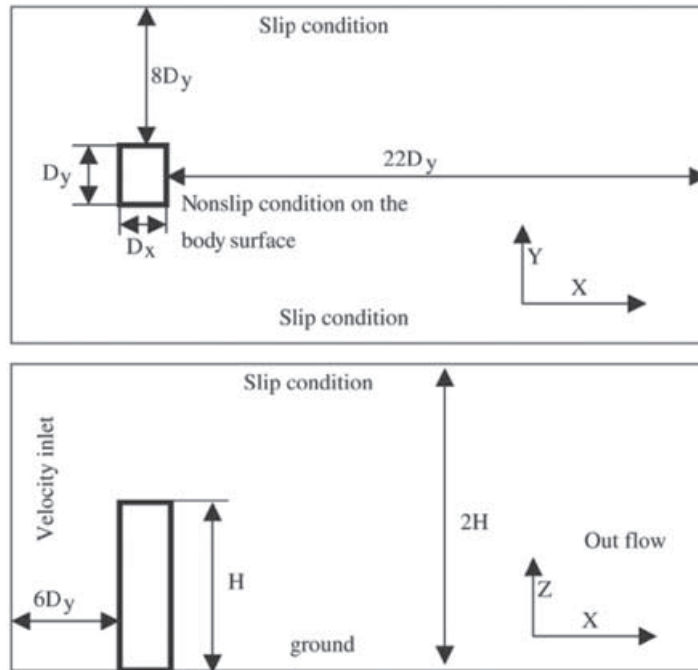
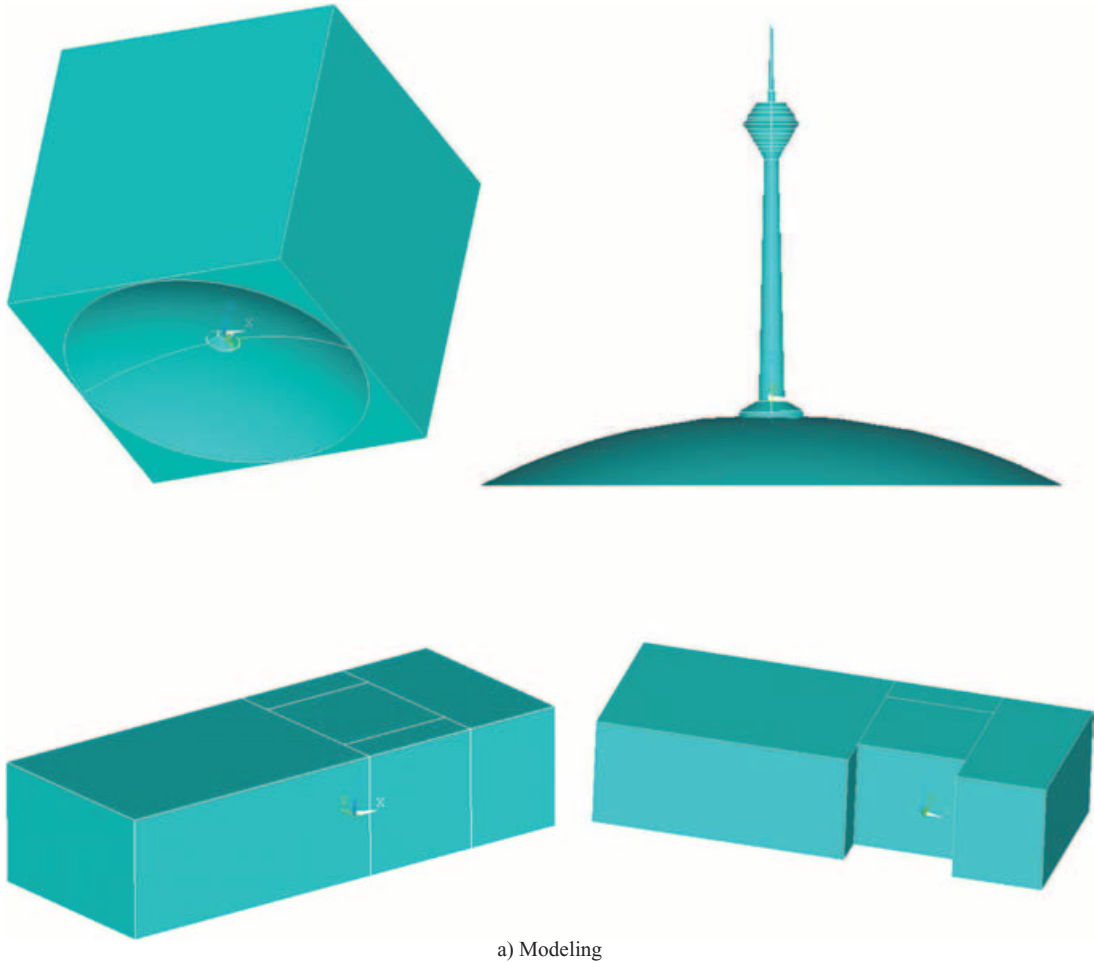


Figure 2. Computational domains and boundary conditions

The primary characteristic of this mesh style is that the tower model is nested in a rectangular cylinder about four times larger than the tower. For zones in the nesting rectangular cylinder, an unstructured mesh is generated, while for zones outside the nesting rectangular cylinder, the structured mesh is applied. This arrangement provides fine mesh in the neighbourhood of the tower surfaces while keeping the mesh in zones far away from the tower surfaces unchanged or in a proper coarser state. Another important advantage of this arrangement is that the mesh aligned with the tower surfaces does not need to be stretched with the wall boundary-layer grid as the structured mesh does. The turbulence model used in this study is the standard $k - \varepsilon$ model. As it was mentioned before, this model is frequently used for simulation of wind flows around bluff bodies, and its advantages and limitations are well described and documented by Murakami (1998).

The transport equations and standard values of the empirical constants involved in the standard $k - \varepsilon$ model adopted in the ANSYS code are the same as the original ones. For the LES model, dynamic SGS kinetic energy model is used in the ANSYS software for SGS approach. The dynamic SGS kinetic energy model describes the SGS turbulence by accounting for the transport of the SGS turbulence kinetic energy, which was found to be more suitable than an algebraic expression based on local equilibrium assumptions given by the Smagorinsky series. The underlying local equilibrium assumption is that equilibrium exists between the transferred energy through the grid-filter scale and the dissipation of kinetic energy at small SGSs. In fact, for high Reynolds number bluff body flows, the local equilibrium assumption is questionable. Therefore, the dynamic SGS kinetic energy model is used in this study. The SGS kinetic energy of the dynamic SGS kinetic energy model is defined as $k_{sgs} = \frac{1}{2}(\overline{U_k^2} - \overline{U_k}^2)$, which is obtained by contracting the SGS stress in $\tau_{ij} = \rho \overline{U_i U_j} - \rho \overline{U_i} \overline{U_j}$. The SGS eddy viscosity, μ_t , is computed using k_{sgs} as $\mu_t = C_k K_{sgs}^{\frac{1}{2}} \Delta_f$, where Δ_f is the filter size computed from



a) Modeling

Figure 3. The (a) modelling and (b) mesh arrangement

$\Delta_f = V \frac{2}{3}$. The SGS stress can then be written as $\tau_{ij} = 2/3 = k_{sgs} \delta_{i,j} - 2\mu_t \overline{S_{i,j}}$ while k_{sgs} is obtained by solving its transport equation:

$$\frac{\partial k_{sgs}}{\partial t} + \frac{\partial U_j \bar{k}_{sgs}}{\partial x_j} = -\tau \frac{\partial \bar{U}}{\partial x_j} - C_\epsilon k_{sgs}^{3/2} + \frac{\partial}{\partial x_j} \left(\frac{\mu_t}{\sigma_k} \frac{\partial k_{sgs}}{\partial x_j} \right) \quad (1)$$

In the above equations, the model constants C_ϵ and C_k are determined dynamically (Kim and Menon, 1997). The parameter δ_k is hard-wired to 1.0.

3.2 Boundary conditions

To obtain the best agreement between the results of the experiment and numerical simulation, boundary condition adopted in the numerical simulation should be the same as those in the experiment,



b) Meshing

Figure 3. *Continued*

especially for inflow boundary condition. The input velocity profile represents mean wind velocity changes by increasing the height level from ground surface in upper fluid flow environment region. There are two kinds of expression to describe the velocity profile of atmospheric boundary layer simulated in wind tunnel tests. One is a power law and the other is a log law. This velocity change is presented by logarithmic and power laws by Equations (2) and (3), respectively.

$$u(y) = \bar{u}_{ABL} \ln\left(\frac{y}{y_r}\right) \quad (2)$$

$$u(y) = \bar{u}_{ABL} \left(\frac{y}{y_r}\right)^\alpha \quad (3)$$

where \bar{U}_{ABL} is the reference mean velocity, y is the height from the ground, y_r is the reference height and α is the power of velocity profile. According to ASCE provisions (ASCE) and the

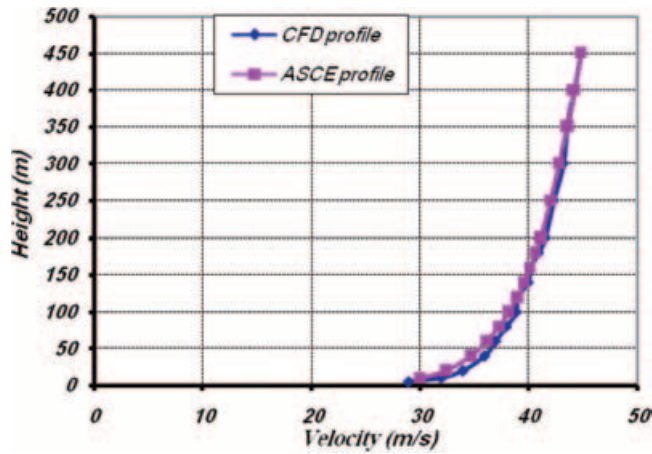


Figure 4. Applied velocity profile

environmental conditions of the region in which the Milad tower is located, in wind tunnel test, the reference height, power coefficient and reference wind speed were considered to be 10, 0.11 and 30 m/s, respectively. In the numerical study, these values are also used. The applied velocity profile is shown in Figure 4

As discussed by Li and Melbourne (1999a, 1999b), turbulence intensity in the approaching flow has a significant effect on the stream-wise distributions of wind-induced pressures on building models; hence, the turbulence intensity profile should be properly modelled for obtaining accurate simulation results. Turbulence kinematic energy and its dissipation rate in input are calculated by the following equations:

$$K(y) = \frac{U_{ABL}^{*2}}{\sqrt{C_\mu}} \quad (4)$$

$$\varepsilon(y) = \frac{U_{ABL}^{*3}}{ky} \quad (5)$$

where U_{ABL}^* is the frictional velocity and k is the von Karman's constant assumed to be between 0.4 and 0.42. Turbulence profiles for open ground with $U^* = 1$ m/s are presented in Figure 5.

In the LES study, apart from the mean velocity profile, information on the fluctuating velocity of incident wind is also needed. The spectral synthesizer in the ANSYS code was used to generate fluctuating velocity components, which are based on the random flow generation technique modified by Smirnov *et al.* (2001). In this method, fluctuating velocity components are computed by synthesizing a divergence-free velocity vector field from the summation of Fourier harmonics on the basis of the input turbulence boundary conditions.

4. RESULTS AND DISCUSSIONS

4.1 Numerical calibration

Drag- and lift-force coefficients and root mean square values for various cases are compared with the available experiment data, as shown in Table 1. The detailed definitions of these coefficients are given

EFFECT OF WIND ON MILAD TOWER

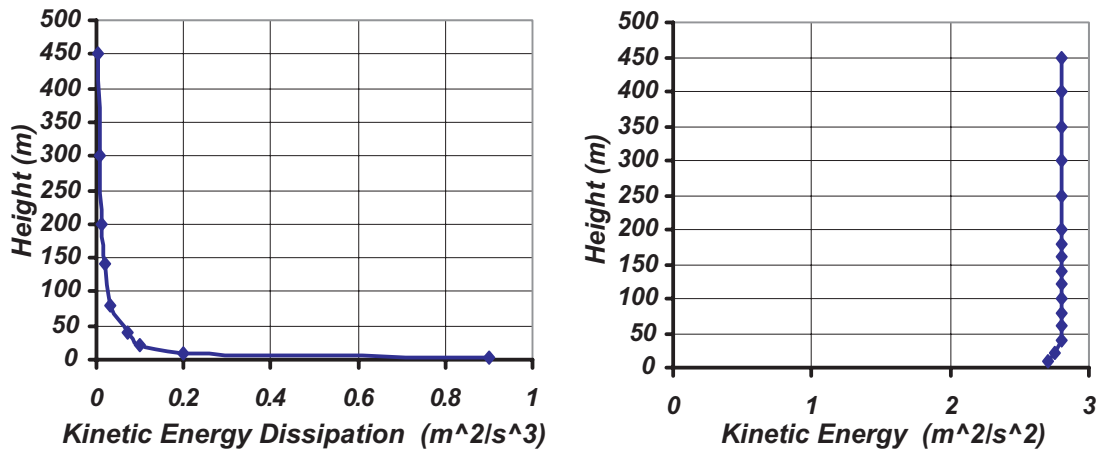


Figure 5. Turbulence profiles

Table 1. Comparison of the results from different calculation methods and experiments ($\alpha = 0$)

Case Number	Turbulence model	C_D	$C_{\sigma_{Fx}}$	C_L	$C_{\sigma_{Fy}}$
1	Standard $k - \epsilon$	1.35	0.0001	0.009	0.02691
2	Dynamic SGS kinematic energy LES	1.71	0.116	0.0036	0.28062
Experimental data		1.611	0.269	0	0.3

SGS, subgrid scale; LES, large eddy simulation.

in Appendix A. By comparing the values presented in Table 1, it can be concluded that, as expected, the standard $k - \epsilon$ model under-predicts the drag-force coefficient C_D by about 20% and gives almost a zero value of $C_{\sigma_{Fy}}$, $C_{\sigma_{Fx}}$, indicating that the wind flow predicted by the standard $k - \epsilon$ model is in steady state. This contradicts the assumed Reynolds number range.

The LES does give the right answers for all the coefficients except the under-prediction of $C_{\sigma_{Fx}}$ by 50% and the slight over-prediction of the drag-force coefficient.

The under-prediction may be caused by short average time due to the limitation of the computational resources.

In the wind tunnel test carried out on the Milad tower, the value of pressure is measured in the tower points shown in Figure 6. To verify the results of the numerical calculation, the pressure coefficients obtained by the test and numerical modelling are compared for these points, and in Figure 7, the values of C_p obtained by numerical calculations are compared with those of tunnel wind test in positions 3, 6 and 15.

As it can be seen in Figure 7, results of the numerical method are in the range of experimental results, and there is a good agreement between results of the numerical method and results of the experimental test. But as it can be seen, comparing with results from the RANS model, the computed pressure distribution from the LES is closer to those obtained from model tests. The $k - \epsilon$ model overestimates pressure values due to inaccurate prediction of turbulence in the contact region in the windward surface. Since there are some differences between the results of numerical calculation and wind tunnel test at front, side and back surfaces, the following conclusions may be present.

The difference in pressure coefficient in the windward surface is much less than those in other surfaces. It seems that the measurement of surface pressures in the windward surface is less affected by the factors such as blockage ratios, simulated boundary layer and turbulence characteristics.

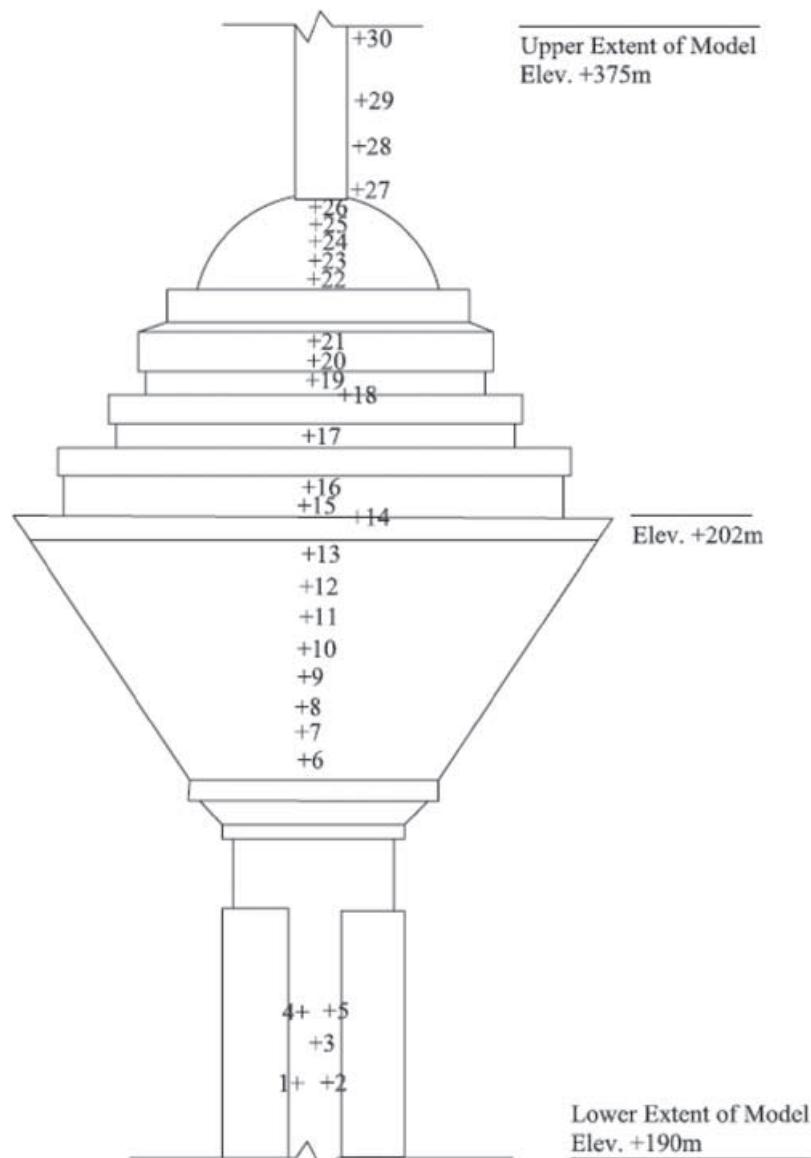


Figure 6. The pressure measurement points in wind tunnel test

In contrast to the front surface, the results of the $k - \varepsilon$ model are more underestimated than those of the LES model.

In side surfaces, although the predicted values by numerical simulation are approximately the same, the predicted pressure distribution patterns by the standard $k - \varepsilon$ model and LES model are different.

4.2 Flow field investigation

Flow patterns obtained by numerical studies are shown in Figure 8. The flow patterns are close in the general form, and the calculated values are close to the real ones. The negligible differences between

EFFECT OF WIND ON MILAD TOWER

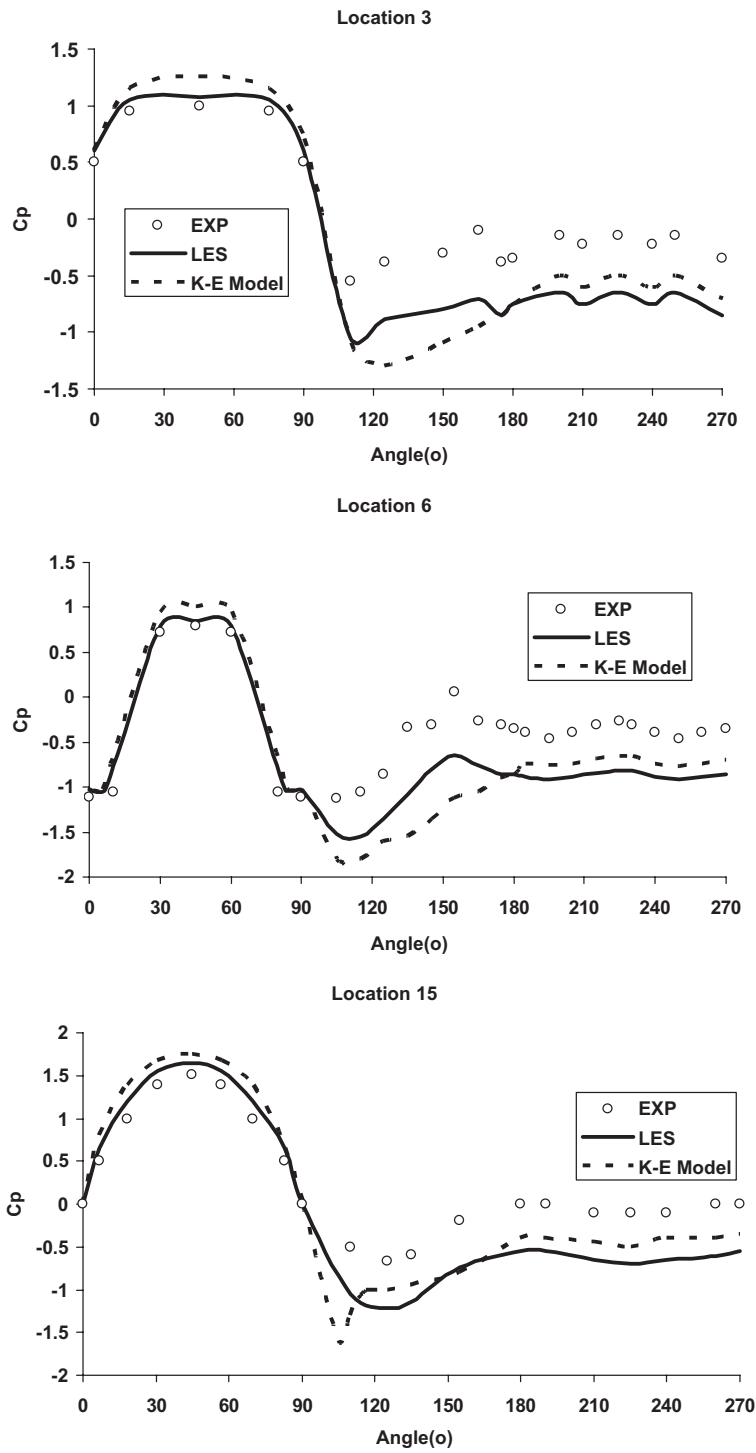


Figure 7. Maximum pressure coefficient in positions 3, 6 and 15

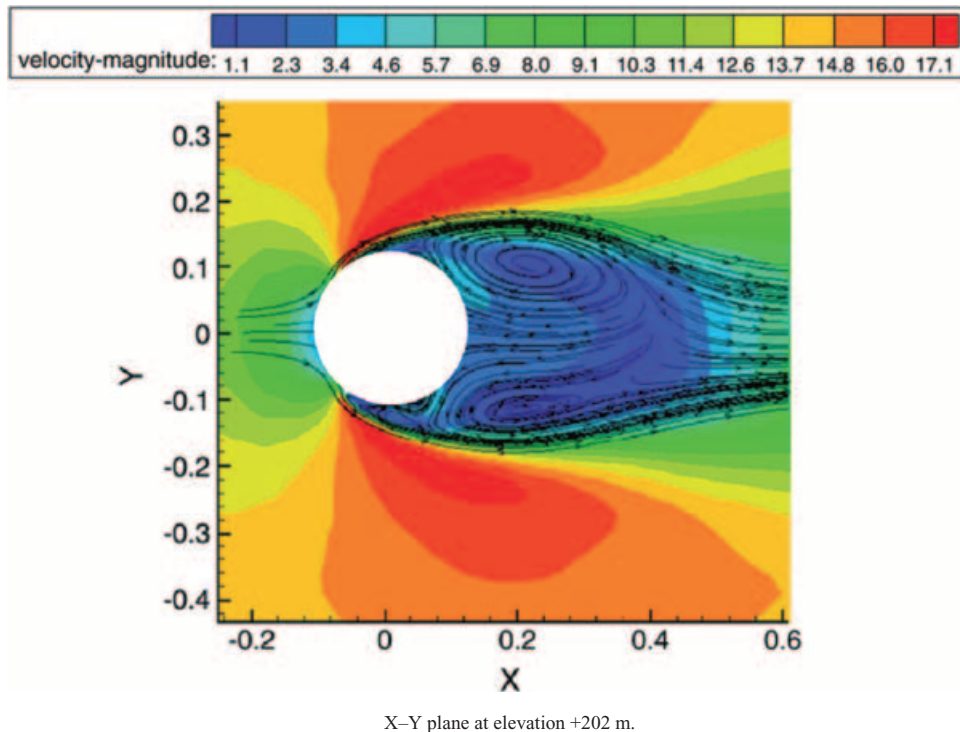


Figure 8. Mean velocity contour distributions

the obtained results and the real ones are due to the difference in the assumed boundary-layer condition.

To decrease these differences, condition of boundary layers should be simulated more accurately by accurate investigations. Predictions of turbulence viscosity by RANS model are drawn in Figure 9. It is observed that the turbulence is over-predicted by the standard $k - \varepsilon$ model, and an unrealizable turbulence ratio is calculated in the impinging region and wake region. The over-predicted turbulent viscosity results in the prediction of a small separation bubble but large and downstream arch vortex prediction.

5. CONCLUSION

Numerical simulation results of wind effects on the Milad telecommunication tower in atmospheric boundary layers with Reynolds number larger than 10^5 have been presented in this paper. The effectiveness of the turbulence models and numerical treatments for solving the practical problem with a high Reynolds number was investigated in detail. Considering the results of this study, the following conclusions are obtained.

Among the concerned turbulence models, the LES with a dynamic SGS model can provide satisfactory predictions for the mean pressure coefficients and reasonable results of fluctuating pressure coefficients for this tower.

The RANS model with standard turbulence model can present acceptable results and have the advantage of providing fast solutions.

Flow field around the tower can be simulated and studied by CFD analysis.

EFFECT OF WIND ON MILAD TOWER

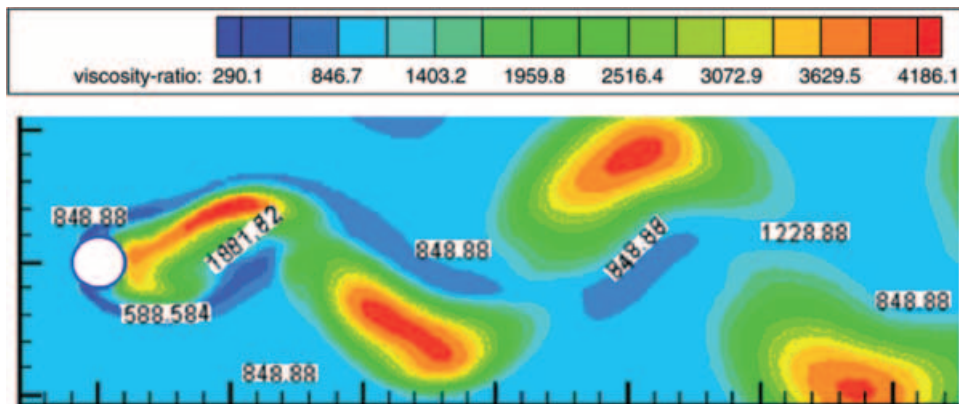


Figure 9. Turbulent viscosity ratio contour

Although the comparison between numerical simulation and experimental tests shows good agreement, to improve CFD techniques, many subjects can be studied, including grid-generation strategies for complex solution domain, application of a higher order of numerical schemes for space and time discrimination, more general and reliable SGS turbulence models for the LES, more accurate and realistic methods for generation of inflow boundary turbulence characteristics, etc.

REFERENCES

- ASCE. Provision for Minimum Design Loads for Buildings and other structures. ASCE 7-98, Wind Loading on Structures.
- Germano M, Piomelli U, Moin P, Cabot WH. 1991. A dynamic subgrid-scale eddy viscosity model. *Physics of Fluids* **A3**(7): 1760–1765.
- Kim WW, Menon S. 1997. Application of the localized dynamic subgrid-scale model to turbulent wall-bounded flows. *Technical report AIAA-97-0210*, American Institute of Aeronautics and Astronautics, 35th Aerospace Sciences Meeting, Reno, NV.
- Lauder BE, Kato M. 1993. *Modeling Flow-Induced Oscillations in Turbulent Flow around a Square Cylinder*. ASME Fluid Engineering Conference: USA.
- Li QS, Melbourne WH. 1999a. Turbulence effects on surface pressures of rectangular cylinders. *Wind and Structures, An International Journal* **2**(4): 253–266.
- Li QS, Melbourne WH. 1999b. The effects of large scale turbulence on pressure fluctuations in separated and reattaching flows. *Journal of Wind Engineering and Industrial Aerodynamics* **83**: 159–169.
- Li QS, Fang JQ, Jeary AP, Paterson DA. 1998. Computation of wind loading on buildings by CFD. *Hong Kong Institution of Engineers, Transactions* **5**(3): 51–70.
- Lilly DK. 1992. A proposed modification of the Germano subgrid-scale closure model. *Physics of Fluids* **4**: 633–635.
- Murakami S. 1998. Overview of turbulence models applied in CWE-1997. *Journal of Wind Engineering and Industrial Aerodynamics* **74–76**: 1–24.
- Murakami S, Mochida A, Kondo K, Ishida Y, Tsuchiya M. 1998. Development of new $k - \epsilon$ model for flow and pressure fields around bluff body, CWE96, Colorado, USA, 1996. *Journal of Wind Engineering and Industrial Aerodynamics* **67–68**: 169–182.
- Nicoud F, Ducros F. 1999. Subgrid-scale stress modeling based on the square of the velocity gradient tensor. *Flow, Turbulence and Combustion* **62**(3): 183–200.
- Rodi W. 1997. Comparison of LES and RANS calculations of the flow around bluff bodies. *Journal of Wind Engineering and Industrial Aerodynamics* **69–71**: 55–75.
- Smagorinsky J. 1963. General circulation experiments with the primitive equations: I. the basic experiment. *Monthly Weather Review* **91**: 99–164.
- Smirnov R, Shi S, Celik I. 2001. Random flow generation technique for large eddy simulations and particle-dynamics modeling. *Journal of Fluids Engineering* **123**: 359–371.

APPENDIX A: DEFINITIONS OF THE FORCE AND PRESSURE COEFFICIENTS

The drag and transverse force coefficients C_D and C_L are defined as

$$C_D = \frac{F_D}{\frac{1}{2} \rho D_y \int_0^H U^2 dZ}, C_L = \frac{F_L}{\frac{1}{2} \rho D_y \int_0^H U^2 dZ} \quad (A1)$$

where ρ is the fluid density and U is the steady part of the longitudinal component of the undisturbed wind velocity at height Z . F_D and F_L are the steady forces acting parallel and transverse to the along-wind direction, respectively. $\int_0^H U^2 dZ$ is defined to account for the wind shear profile, and for the inlet velocity profile given by Equation (A2), one has

$$\int_0^H U^2 dZ \approx 0.7315 U_H^2 H \quad (A2)$$

For the inlet velocity profile given by Equation (A4), we have

$$\int_0^H U^2 dZ \approx 0.625 U_H^2 H \quad (A3)$$

and

$$C_{\sigma F_x} = \frac{\sigma_{F_x}}{\frac{1}{2} \rho U_H^2 D_y H}, C_{\sigma F_y} = \frac{\sigma_{F_y}}{\frac{1}{2} \rho U_H^2 D_y H} \quad (A4)$$

The mean pressure coefficient is defined as

$$C_p = 2(p - p_0) / (\rho U^2) \quad (A5)$$

where p is the time mean pressure and p_0 is a reference pressure coefficient. It is chosen as the pressure of a point far away from the building model (it was given the value of 1 atm in this study).